

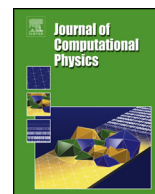


ELSEVIER

Contents lists available at ScienceDirect

Journal of Computational Physics

www.elsevier.com/locate/jcp



Determining the effective resolution of advection schemes. Part II: Numerical testing

James Kent^{a,*}, Christiane Jablonowski^a, Jared P. Whitehead^b, Richard B. Rood^a^a Department of Atmospheric, Oceanic and Space Science, University of Michigan, 2455 Hayward St., Ann Arbor, MI 48109-2143, USA^b Mathematics Department, Brigham Young University, 350 TMCB, Provo, UT 84602, USA

ARTICLE INFO

Article history:

Received 21 March 2014

Received in revised form 14 August 2014

Accepted 26 August 2014

Available online 3 September 2014

Keywords:

Effective resolution

Finite-difference methods

Test case

Dispersion analysis

Dynamical core

ABSTRACT

Numerical models of fluid flows calculate the resolved flow at a given grid resolution. The smallest wave resolved by the numerical scheme is deemed the effective resolution. Advection schemes are an important part of the numerical models used for computational fluid dynamics. For example, in atmospheric dynamical cores they control the transport of tracers. For linear schemes solving the advection equation, the effective resolution can be calculated analytically using dispersion analysis. Here, a numerical test is developed that can calculate the effective resolution of any scheme (linear or non-linear) for the advection equation.

The tests are focused on the use of non-linear limiters for advection schemes. It is found that the effective resolution of such non-linear schemes is very dependent on the number of time steps. Initially, schemes with limiters introduce large errors. Therefore, their effective resolution is poor over a small number of time steps. As the number of time steps increases the error of non-linear schemes grows at a smaller rate than that of the linear schemes which improves their effective resolution considerably. The tests highlight that a scheme that produces large errors over one time step might not produce a large accumulated error over a number of time steps. The results show that, in terms of effective-resolution, there is little benefit in using higher than third-order numerical accuracy with traditional limiters. The use of weighted essentially non-oscillatory (WENO) schemes, or relaxed and quasi-monotonic limiters, which allow smooth extrema, can eliminate this reduction in effective resolution and enable higher than third-order accuracy.

© 2014 Elsevier Inc. All rights reserved.

1. Introduction

Advection schemes perform an important role in the numerical models used for computational fluid dynamics. The advection equation describes passive transport, although many advection schemes can be used to solve conservation laws, such as the density or vorticity equations. They are a key component of a dynamical core, which solves the fluid dynamic equations in weather and climate general circulation models (GCMs). The advection equation is used to transport the many tracer species used in weather and climate studies and is strongly linked to the chemistry module and some subgrid-scale physical parameterizations [11,22].

* Corresponding author. Tel.: +1 734 763 6241.

E-mail addresses: jdkent@umich.edu (J. Kent), cjablono@umich.edu (C. Jablonowski), whitehead@mathematics.byu.edu (J.P. Whitehead), rbrood@umich.edu (R.B. Rood).

<http://dx.doi.org/10.1016/j.jcp.2014.08.045>

0021-9991/© 2014 Elsevier Inc. All rights reserved.

It is well known that the smallest resolved waves of a numerical scheme for the advection equation are often significantly larger than the grid spacing [34]. For weather and climate models this means that many atmospheric features, that are of the order of the grid scale, are not resolved by the model. Determining the smallest resolved wave of an atmospheric model, which we define as the effective resolution, provides insight into which scales are believable [12]. This can be used to determine the grid spacing required to properly represent atmospheric features. Knowledge of the effective resolution of a numerical scheme also informs the coupling of a dynamical core to subgrid scale physical parameterizations, which provide a forcing mechanism at the grid scale. Increasing the effective resolution of a model by using higher-order numerical methods might prove beneficial in terms of cost rather than just increasing the grid resolution (similar to the idea of equivalent resolution [36]).

Part I of our series of papers [8] used dispersion relation analysis to calculate the effective resolution of a number of schemes for the linear advection equation. Dispersion relation and von Neumann analysis are tools that have been used to analyze many numerical methods [14,20,21,24,35]. If a scheme's dispersion properties match those of the governing equation at a given wave number, and within a given error tolerance, then that wave number is classified as resolved [8,32].

One drawback of the dispersion analysis is that it can only be applied to linear schemes. For the advection equation there are many different types of numerical schemes (see, for example, [13,23,25]). Many advection schemes contain non-linear components, such as limiters or filling algorithms, and as such the effective resolution of these schemes cannot be assessed by dispersion analysis. Here, we present a numerical test that can be used by both linear and non-linear advection schemes to calculate their effective resolution. The numerical test analyses the method over a number of time steps, which will have an impact on the non-linear schemes, as numerical schemes that perform poorly over a single time step might not produce a large accumulated error over a number of time steps. We use this method to investigate the effect that non-linear components, such as limiters, have on the effective resolution of advection schemes.

The analysis and numerical testing in our paper focuses on the linear advection equation, allowing easy comparison with the dispersion analysis performed by [8]. The advection equation is reviewed in Section 2, along with a recap of the analysis of [8]. In Section 3 we develop idealized numerical tests to allow the calculation of the effective resolution of any advection scheme. Section 4 shows the results from the numerical testing of limited schemes, while Section 5 provides the summary and conclusions.

2. The advection equation and dispersion analysis

The one-dimensional advection equation is given as

$$\frac{\partial q}{\partial t} + u \frac{\partial q}{\partial x} = 0, \tag{1}$$

where $q(x, t)$ is a tracer mixing ratio, u is the velocity (in this paper we choose u constant, with $u = 1$), x is the spatial direction and t is time. Note that all quantities are dimensionless in this paper. The solution to the constant velocity advection equation is known, and is given as

$$q_T(x, t) = q_0(x - ut), \tag{2}$$

where q_0 is the initial tracer and the subscript T indicates the true solution.

The effective resolution describes the smallest wave (largest wave number) that is fully resolved by a numerical scheme. To calculate the effective resolution using dispersion analysis we follow [8]. For the one-dimensional advection equation with constant velocity the true amplitude factor, $|\Gamma|$, and dispersion relation are given as

$$|\Gamma| = 1, \quad \omega = uk, \tag{3}$$

where k is the spatial wave number, and ω is the frequency. To calculate the effective resolution, the scheme's amplitude factor ($|\Gamma_N|$) and dispersion relation (ω_N) are compared with the true amplitude factor and dispersion relation for all wave numbers. The amplitude factor and dispersion relation are calculated by substituting the wavelike solution

$$q_j^n = \hat{q} \exp(i(kx_j - \omega t_n)) \tag{4}$$

into the discretization. Here n and j are the temporal and spatial indices, i is the imaginary unit and \hat{q} is the amplitude. The amplitude factor is calculated as $|\Gamma| = |\exp(-i\omega\Delta t)|$, for a time step Δt . Wave number k is defined as fully resolved if

$$\frac{||\Gamma| - |\Gamma_N||}{|\Gamma|} \leq \epsilon, \quad \frac{|\omega - Re(\omega_N)|}{|\omega|} \leq \epsilon, \tag{5}$$

for all wave numbers $\leq k$ at some error threshold ϵ . Following [8,32], we use $\epsilon = 0.01$, i.e. a scheme must be within 99% of the true amplitude factor and dispersion relation. We are interested in the effective resolution of a scheme as it transports a quantity over the distance of one grid box, Δx . To do this the amplitude factor is taken to the power m , where $m = 1/c$ for Courant number $c = u\Delta t/\Delta x$ (i.e. m is the number of time steps required to transport a quantity one full grid box).

3. Numerically determining effective resolution

To determine the effective resolution of non-linear schemes, numerical testing and an analysis of error norms are required. For consistency with [8], even though the numerical testing advects the tracer over a number of grid boxes, the numerically calculated effective resolution tells us the smallest wave that a numerical scheme can fully resolve over the distance Δx . As with [8] we only consider a uniform grid of equal spacing. Our method involves splitting the numerical error into diffusive and dispersive parts. We then specify an error tolerance to class a wave number as resolved or unresolved. We class wave number k as being resolved if both the diffusive and dispersive errors are less than the error tolerance for all wave numbers less than k .

To create initial conditions of wave number k on the domain $0 \leq x \leq 1$ we use the cosine function

$$q_0 = 1 + \cos(2\pi kx). \tag{6}$$

This function has a minimum value of zero, so it is useable with schemes that have a positivity filter. The solution, after time t , is given as in Eq. (2).

Following [27] the normalized mean square error for tracer solution q_C compared with true solution q_T on a grid with M equally spaced points can be separated into diffusive (DIFF) and dispersive (DISP) parts. First the normalized mean square error is calculated as

$$E = \frac{\sum(q_T - q_C)^2/M}{\sum(q_T)^2/M}, \tag{7}$$

and then the diffusive and dispersive parts are given by

$$E_{DIFF} = \frac{[\sigma(q_T) - \sigma(q_C)]^2 + (\bar{q}_T - \bar{q}_C)^2}{\sum(q_T)^2/M}, \tag{8}$$

where σ is the standard deviation and the overbar signifies the spatial mean, and

$$E_{DISP} = E - E_{DIFF}. \tag{9}$$

We specify the tolerance, $(\epsilon_{DIFF}, \epsilon_{DISP})$, and define wave number k as being unresolved by a given numerical scheme if

$$E_{DIFF} > \epsilon_{DIFF} \quad \text{or} \quad E_{DISP} > \epsilon_{DISP}. \tag{10}$$

The test is repeated for all positive integers $k \leq M/2$ until a wave number is classed as unresolved.

3.1. Threshold values

This method is designed to numerically calculate the effective resolution of an advection scheme. We require that the results are reproducible independent of the grid resolution. For example, if a scheme resolves wave number 4 on a grid with 128 grid points, the scheme must also resolve wave number 8 on a grid with 256 grid points (as they represent the $32\Delta x$ wave on the different grids). Also, we require that our method produces the same results for linear schemes regardless of the number of time steps used, i.e. the results for linear schemes are not dependent on the number of grid boxes the quantity is advected over during a simulation. This means that even if we use our scheme to advect q over two grid boxes, the test method will produce the same results as if we had advected q over one box. We specify G as the number of grid cells that the tracer will be advected across during the simulation (i.e. the tracer is therefore transported a distance $G\Delta x$).

First we consider the diffusive errors. The profile

$$q_{df} = 1 + (1 - \epsilon) \cos(2\pi kx), \tag{11}$$

will have the same phase as the initial condition q_0 (6) for a given k , but the amplitude of q_{df} will only be $(1 - \epsilon)$ of q_0 . We can calculate ϵ_{DIFF} analytically by considering the continuous case, i.e. the summations in the error calculation (7) become integrals over the domain, and using $q_T = q_0$ and $q_C = q_{df}$. For q_{df} we have $E_{DISP} = 0 \Rightarrow E_{DIFF} = E$, therefore we just need the normalized mean square error (7). The denominator becomes

$$\int_0^1 (q_0)^2 dx = \int_0^1 (1 + \cos(2\pi kx))^2 dx = \frac{3}{2}. \tag{12}$$

The numerator of the normalized mean square error is

$$\begin{aligned} \int_0^1 (q_0 - q_{df})^2 dx &= \int_0^1 [1 + \cos(2\pi kx) - 1 - (1 - \epsilon) \cos(2\pi kx)]^2 dx \\ &= \left[\left(\frac{x}{2} + \frac{\sin 4\pi kx}{8\pi k} \right) \epsilon^2 \right]_0^1 \\ &= \frac{\epsilon^2}{2}. \end{aligned} \tag{13}$$

Combining the numerator with the denominator we get that the threshold value is

$$\epsilon_{DIFF} = \frac{\epsilon^2}{3}. \quad (14)$$

For consistency with [8] we set $\epsilon = 0.01$, which means that q_{df} has a 1% diffusive error. This gives our threshold $\epsilon_{DIFF} = 1/30000$ for $G = 1$. Numerically calculating E_{DIFF} using (8) for q_{df} confirms this value for any wave number k .

Next we consider the dispersive error. If we transport a quantity over the distance Δx , then we consider a wave to be completely out of phase if it has not moved. Therefore the profile

$$q_{ds} = 1 + \cos(2\pi k(x - \epsilon \Delta x)), \quad (15)$$

will have the same amplitude as q_0 , but the phase will only be $(1 - \epsilon)$ of q_0 . We calculate ϵ_{DISP} using the continuous case with $q_t = q_0$ and $q_c = q_{ds}$, and the denominator from (12). For q_{ds} we have $E_{DIFF} = 0 \Rightarrow E_{DISP} = E$. The numerator of (7) becomes

$$\begin{aligned} \int_0^1 (q_0 - q_{ds})^2 dx &= \int_0^1 [1 + \cos(2\pi kx) - 1 - \cos(2\pi k(x - \epsilon \Delta x))]^2 dx \\ &= \int_0^1 \cos^2(2\pi kx) + \cos^2(2\pi k(x - \epsilon \Delta x)) dx \\ &\quad - 2 \int_0^1 \cos(2\pi kx) \cos(2\pi k(x - \epsilon \Delta x)) dx \\ &= 1 - 2 \int_0^1 \cos(2\pi kx) \cos(2\pi k(x - \epsilon \Delta x)) dx \\ &= 1 - \int_0^1 \cos(2\pi kx) + \cos(2\pi k(2x - \epsilon \Delta x)) dx \\ &= 1 - \int_0^1 \cos(2\pi k\epsilon \Delta x) + \cos(2\pi k(2x - \epsilon \Delta x)) dx \\ &= 1 - \cos(2\pi k\epsilon \Delta x). \end{aligned} \quad (16)$$

Using the first two terms of the Taylor series expansion of the cosine term, the numerator can be approximated as

$$1 - \left(1 - \frac{(2\pi k\epsilon \Delta x)^2}{2}\right) = \frac{(2\pi k\epsilon \Delta x)^2}{2}. \quad (17)$$

Combining with the denominator, the dispersive threshold is

$$\epsilon_{DISP} = \frac{(2\pi k\epsilon \Delta x)^2}{3}. \quad (18)$$

This means that the dispersive threshold is dependent on the wave number k . Setting $\epsilon = 0.01$, i.e. q_{ds} has a 1% dispersive error, and rewriting the wave number in terms of $N\Delta x$ gives $\epsilon_{DISP} \approx 0.00132/N^2$ for $G = 1$. Numerically calculating E_{DISP} using (9) confirms the dispersive threshold.

The next point to consider is the case of $G \neq 1$. For a given Courant number c , the number of time steps to run the simulation, G/c , must be an integer. Therefore $G = 1$ would not be admissible for $c = 0.6$ for example, and another value, e.g. $G = 0.6$ or $G = 6$, must be used. (Note that while G/c must be an integer, G doesn't have to be an integer.) As the error measures, Eqs. (7)–(9), are based on the mean square error, the error for linear schemes will grow proportional to the number of time steps squared. This is the case for the forward-in-time schemes (see Section 4.1) at large scales e.g. a wavelength of $N = 32\Delta x$. However, as the scales decrease and tend to $2\Delta x$, the errors lose the time step squared dependence for simulations over a large number of time steps. This is because the schemes reach their maximum error over fewer steps (for example, a predominantly diffusive scheme will diffuse the tracer to $q = 1$ at all grid points, and therefore the error is unable to grow). Numerical testing (not shown) indicates that the linear schemes' errors maintain the time step squared dependence for the large scales for more than 100 time steps.

A final point for the diffusive errors is that for $G = 2$, the error measure is not equivalent to $\epsilon = 0.02$, i.e. a 2% error. A scheme that is unresolved will damp the wave by 1% over one grid box, and therefore will damp the wave by 1% of a 1%

damped wave over two grid boxes (and so on for more grid boxes). This is due to the diffusion being applied iteratively. Therefore we consider $G_p = 100 \times (1 - 0.99^G)$ instead of just G when calculating the diffusive error threshold.

From this analysis we find that the threshold values for the diffusive and dispersive errors are

$$\epsilon_{DIFF} = 0.0000\dot{3}G_p^2, \quad \epsilon_{DISP} = \frac{0.00132}{N^2}G^2, \tag{19}$$

respectively (note that the dot signifies a recurring decimal, and ϵ_{DISP} is the approximate rounded value of (18)). Once a scheme’s diffusive or dispersive error exceeds this threshold for wave number k , we say that wave number k is unresolved corresponding to $\epsilon = 0.01$ for the analytic case. This method works well, see Section 3.2, but there are a few caveats. Firstly, the accuracy of the method increases as the number of grid points increases, i.e. using $M = 256$ will more accurately determine which waves are resolved than using $M = 128$. This is because there are more wave numbers available to test using the grid with more points. Secondly, the accuracy of the test decreases as the number of grid boxes to advect across increases, i.e. using $G = 1$ will produce more accurate results than $G \gg 1$. Over a long simulation (very large G) a scheme’s diffusive error may completely smooth the tracer to $q = 1$, thus the diffusive and dispersive errors will not grow over more time steps. Section 3.2 shows that using 100 time steps still produces accurate results.

Finally, we must consider the error of non-linear schemes. For linear schemes the error generally maintains the number of time steps squared dependence, as the linear scheme is applying the same error repeatedly, but this is not true for non-linear schemes. For the case of $\epsilon = 0.01$ we require that the diffusive error must be within 99% of the true value over one grid box, and this corresponds to being within 90.44% of the true value over a distance of ten grid boxes. However, it is possible for a non-linear scheme to be outside 99% over one grid box, but be within 90.44% over ten grid boxes; i.e. the wave number would be classed as unresolved by the scheme over one grid box but resolved over ten grid boxes. A similar argument can be made for dispersion errors. Using $G = c$ will show how the scheme performs over the first time step, which may be significantly different to how the scheme behaves over several steps. Therefore non-linear schemes need to be tested for a variety of G to show the effective resolution due to the behavior of the scheme over different length simulations.

3.2. Comparison to analytical method

To show the validity of our numerical test, we compare the numerical effective resolution with the analytical effective resolution calculated in [8] for a number of schemes. The effective resolution takes into account both the diffusive and dispersive properties of the scheme. For the analytical effective resolution, wave number k is classed as resolved if the scheme’s amplitude factor and dispersion relation at that wave number are both below a given threshold, as in Eq. (5). For the numerical effective resolution, wave number k is classed as resolved if the scheme’s diffusive and the dispersive errors are both less than their respective thresholds, given in Eq. (19), for the initial profile of that wave number. We make use of the forward-in-time schemes of order 1–6 (also known as Lax–Wendroff or ADER schemes [15,30,31]) and the Piecewise Parabolic Method (PPM [2]) with fourth- and sixth-order edge reconstruction and no limiters. These schemes are described in more detail in Section 4.1. We also show results for the fourth-order Runge–Kutta [4] with both second- and fourth-order spatial derivatives.

Fig. 1 shows the effective resolution, in terms of $N\Delta x$, calculated using both the analytical method of [8] and the new numerical methodology, for linear schemes. The numerical effective resolution, calculated using a grid with 1024 points, is measured over 1 time step (i.e. $G = c$), and over 100 time steps ($G = 100c$). Courant numbers at intervals of 0.1 ranging from 0.1 to 1.0 are used. For each of the schemes, our numerical methodology is a very good approximation of the analytical method for calculating the effective resolution (the center and right hand plots of Fig. 1 are very similar to the left plots). The largest difference between the numerical and analytic effective resolutions is less than $2\Delta x$. The results also show that while the 100 time step simulation is still a good approximation to the analytical values, it is less accurate than the 1 time step simulation, as illustrated by the fourth-order forward-in-time scheme at $c = 0.7$.

4. Numerical testing of advection schemes

We use our method to calculate the effective resolution of non-linear schemes applied to the linear advection equation. All the schemes used in this paper are discussed in Section 4.1, and the results of the testing are in Section 4.2.

4.1. List of numerical schemes

The Lax–Wendroff/forward-in-time/ADER schemes [15,30,31] are different methods that produce the same discretization for the constant velocity linear advection equation. The general idea is to use the Taylor series expansion

$$q_j^{n+1} = q_j^n + \Delta t q_t + \frac{\Delta t^2}{2!} q_{tt} + \frac{\Delta t^3}{3!} q_{ttt} + \dots \tag{20}$$

where the derivatives are calculated at time step n and spatial point j . The temporal derivatives are then written in terms of spatial derivatives, for example $q_t = -uq_x$ and $q_{tt} = u^2q_{xx}$, etc., and substituted back into (20). These derivatives are

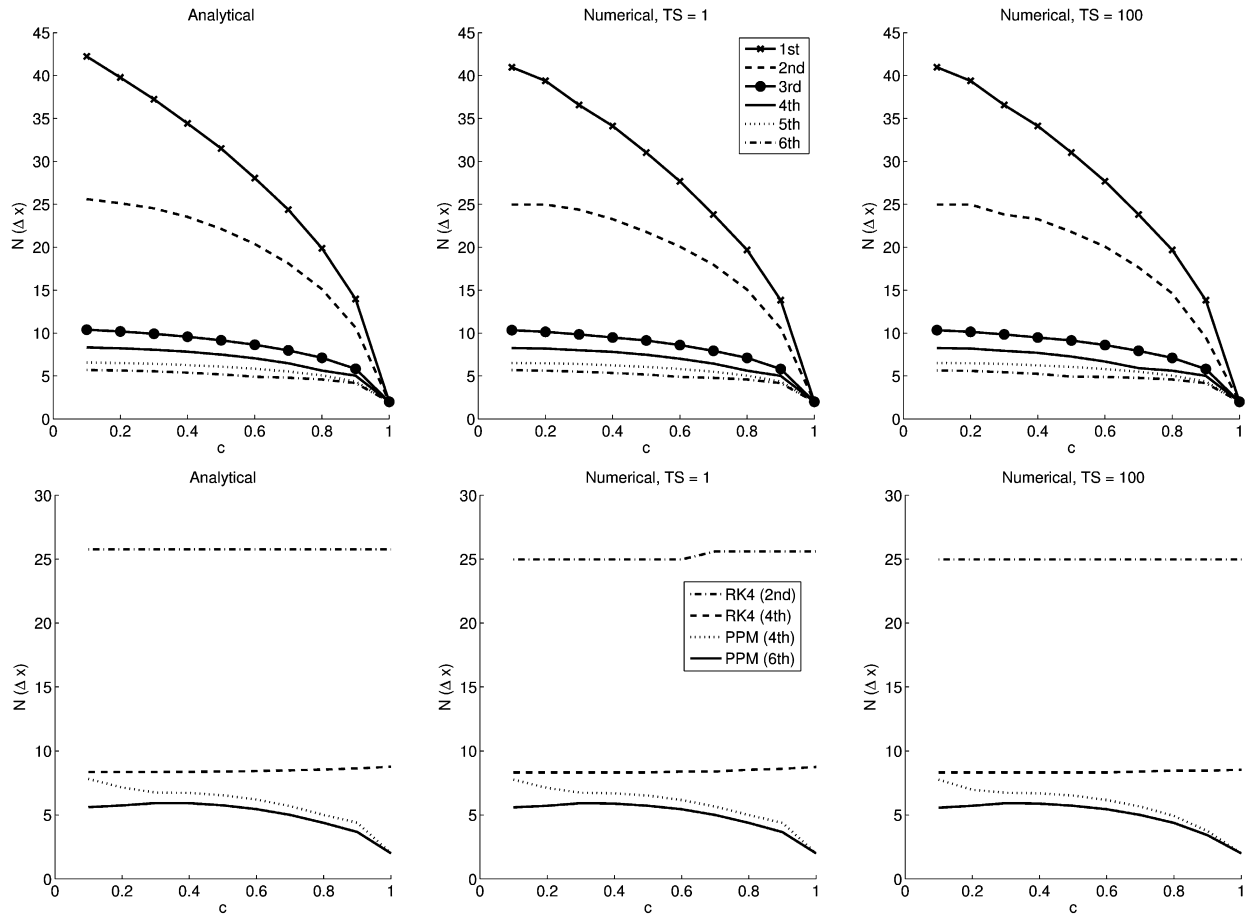


Fig. 1. Comparing the analytical effective resolution (left) with the numerically calculated effective resolution (center and right) for the forward-in-time schemes of order 1–6 (top) and the fourth-order Runge–Kutta with second and fourth-order spatial derivatives (RK4 (2nd) and RK4 (4th) respectively), and unlimited PPM with fourth- and sixth-order edge reconstruction (PPM (4th) and PPM (6th) respectively) (bottom). The plots show the smallest resolved wave in terms of $N\Delta x$ against Courant number c . The number of time steps (TS) is 1 (center) and 100 (right), leading to $G = c$ (center) and $G = 100c$ (right).

calculated using the required order-of-accuracy; this produces a scheme that has the same temporal and spatial order-of-accuracy. These schemes can easily be discretized in flux form. We make use of order 1–6; the first-order version is just the first-order upwind scheme and the second-order version corresponds to the Lax–Wendroff scheme. The ADER method is a finite-volume method that makes use of the flux form of the equation and usually utilizes a limiter. A similar expansion to (20) is used in the flux calculation. For constant velocity advection and without the use of limiters the ADER schemes are equivalent to the Lax–Wendroff and higher-order schemes. For the purposes of this paper we refer to these schemes collectively as ‘forward-in-time’ schemes of order 1–6.

To investigate non-linear schemes we make use of schemes with limiters. Limiters are used to ensure monotonicity and to prevent spurious oscillations occurring in the solution. We consider the van Leer (VL) limiter [33] which can be applied to the second-order Lax–Wendroff scheme. The flux limiter ϕ is a function of successive gradients [26], and is used in conjunction with a high-order flux F^H (in this case the second-order Lax–Wendroff) and a low-order monotonic flux (in this case the first-order upwind scheme). The flux is calculated as

$$F_{j+\frac{1}{2}} = F_{j+\frac{1}{2}}^L + \phi_{j+\frac{1}{2}}(F_{j+\frac{1}{2}}^H - F_{j+\frac{1}{2}}^L). \quad (21)$$

We also consider the Flux-Corrected-Transport (FCT) method of [1]. FCT starts with the first-order upwind scheme and determines how much of an anti-diffusive flux can be added to still produce a monotonic solution. The FCT algorithm can be used with any order scheme to produce the anti-diffusive flux, therefore we have used it with the second-to-fifth order forward-in-time schemes. The universal limiter [16,17], denoted FL, is a flux limiter that can be applied to any high-order flux. Again we apply it to the second-to-fifth order forward-in-time schemes. The universal limiter can be relaxed to allow small over- and under-shoots and therefore higher-order accuracy for smooth data. This procedure is explained in Appendix A, and the relaxed limiter is denoted RL.

Table 1

List of one-dimensional numerical schemes used in this paper. 'Limiter' indicates the use of non-linear limiters and 'Ref' provides the primary reference(s).

Abbr.	Scheme	Limiter	Ref
1st	1st-Order Forward-In-Time (Upwind)	no	
2nd	2nd-Order Forward-In-Time (Lax–Wendroff)	no	[15]
3rd	3rd-Order Forward-In-Time (ADER)	no	[30,31]
4th	4th-Order Forward-In-Time (ADER)	no	[30,31]
5th	5th-Order Forward-In-Time (ADER)	no	[30,31]
VL	Van-Leer (Lax–Wendroff basic)	yes	[33]
FL 2nd	Universal Limiter (Lax–Wendroff basic)	yes	[16,17]
FL 3rd	Universal Limiter (3rd-Order basic)	yes	[16,17]
FL 4th	Universal Limiter (4th-Order basic)	yes	[16,17]
FL 5th	Universal Limiter (5th-Order basic)	yes	[16,17]
RL 2nd	Relaxed-Universal Limiter (Lax–Wendroff basic)	yes	[16,17]
RL 3rd	Relaxed-Universal Limiter (3rd-Order basic)	yes	[16,17]
RL 4th	Relaxed-Universal Limiter (4th-Order basic)	yes	[16,17]
RL 5th	Relaxed-Universal Limiter (5th-Order basic)	yes	[16,17]
FCT 2nd	Flux-Corrected Transport (Lax–Wendroff basic)	yes	[1]
FCT 3rd	Flux-Corrected Transport (3rd-Order basic)	yes	[1]
FCT 4th	Flux-Corrected Transport (4th-Order basic)	yes	[1]
FCT 5th	Flux-Corrected Transport (5th-Order basic)	yes	[1]
PPM 4th	Piecewise Parabolic Method 4th-order edge reconstruction	no	[2]
PPM LIM	Piecewise Parabolic Method 4th-order edge reconstruction	yes	[2]
PPM 6th	Piecewise Parabolic Method 6th-order edge reconstruction	no	[2,3]
PPM 6th LIM	Piecewise Parabolic Method 6th-order edge reconstruction	yes	[2,3]
WENO 4th	4th-Order WENO	yes	[19]
WENO 5th	5th-Order WENO	yes	[7]
RK4 (2nd)	Runge–Kutta 4 with 2nd-order centered difference	no	[4]
RK4 (4th)	Runge–Kutta 4 with 4th-order centered difference	no	[4]

The final schemes we test are non-oscillatory schemes based on the Piecewise Parabolic Method (PPM, [2]) and Weighted Essentially Non-Oscillatory schemes (WENO, [19]). PPM is a finite-volume method that reconstructs a grid cell edge. This edge value is limited to make the reconstruction piecewise and discontinuous. A parabolic subgrid distribution is then calculated using the limited edge reconstruction. We make use of both the limited and unlimited versions of PPM (the unlimited versions are shown in Fig. 1). Due to the parabolic subgrid distribution, unlimited PPM is third-order accurate provided the edge reconstruction is at least third-order. We use two versions; the fourth-order edge reconstruction, which is more typical for PPM, and a sixth-order version given by [3]. WENO schemes are weighted versions of Essentially Non-Oscillatory schemes (ENO, [6]), and use a combination of ENO reconstructions (instead of just the smoothest). They are essentially non-oscillatory, which permits high-order accuracy but does not guaranteed the solution to be monotonic (similar to the relaxed limiter described above). We use the fourth-order [19] and fifth-order versions [7]. A list of all the numerical schemes, including the abbreviation, whether the scheme has a limiter, and the primary reference(s) is found in Table 1.

4.2. Results

The simulations are run for a length of 1, 25, 50 and 100 time steps (i.e. G is 1c, 25c, 50c and 100c) to show the effect of the non-linear schemes over time. The grid is composed of 1024 equally spaced grid points between $0 \leq x \leq 1$. Note that although the accuracy of the method decreases with an increased number of time steps, up to 100 time steps was shown to be satisfactory in Fig. 1. We calculate the effective resolution at Courant numbers at intervals of 0.05 that range from 0.05 to 1.0.

To investigate the effect of limiters on effective resolution, we compare a number of second-order schemes. Fig. 2 shows the comparison between the van Leer, FCT and the universal limiter (FL) applied to the second-order forward-in-time (i.e. Lax–Wendroff) scheme. The second-order unlimited forward-in-time scheme (Lax–Wendroff) is also shown (solid black line). Initially the limiters introduce large diffusion and dispersion errors, as they damp the peaks of the waves. Therefore, over one time step the limited schemes perform poorly when compared with the unlimited scheme. The effective resolution of the limited schemes (VL, FCT and FL) are approximately two times worse than the unlimited second-order scheme over one time step. As the simulation progresses the limited schemes' errors increase at a different rate to the unlimited scheme. As the number of time steps increases, the effective resolution of the limited schemes improves, and after 25 steps the limited schemes start to outperform the unlimited scheme.

The effective resolution when using limiters with a higher-order scheme is shown in Fig. 3. The universal limiter is applied to the second-, third-, fourth- and fifth-order forward-in-time schemes. As with Fig. 2, over one time step the limiter introduces large errors and the effective resolution for each of the schemes is significantly worse than the corresponding unlimited scheme (shown in Fig. 1). Again, as the number of time steps increases the effective resolution of the limited schemes improves. In general, the limited second-order scheme resolves less than the limited third-, fourth- and fifth-order schemes, and less than the second-order unlimited scheme. The effective resolution of the third-, fourth- and fifth-order limited schemes are very similar. This is because the universal limiter damps the peaks of smooth waves and is unable

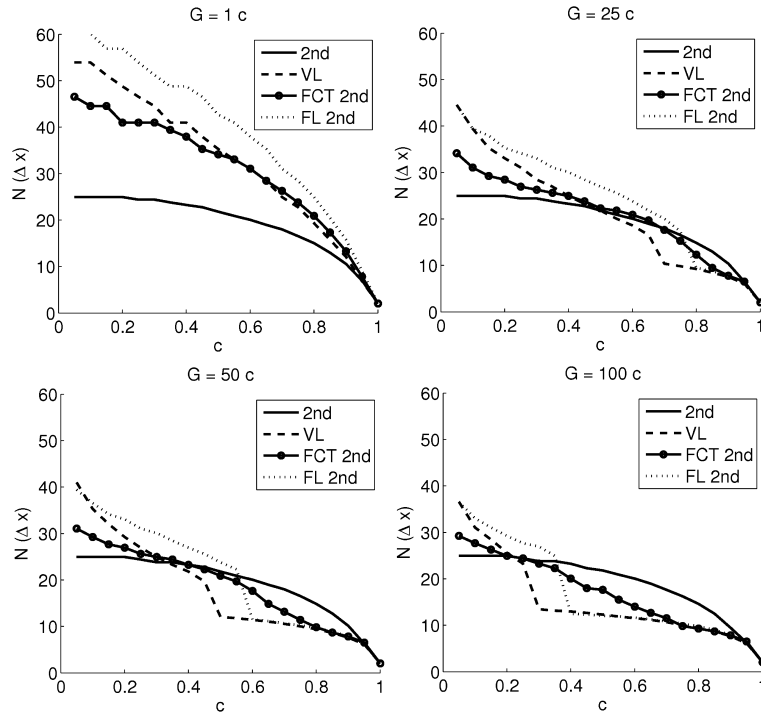


Fig. 2. Numerically calculated effective resolution, in terms of $N\Delta x$, against Courant number c , for the second-order forward-in-time (2nd), van Leer (VL), flux-corrected transport (FCT 2nd) and the universal flux-limited (FL 2nd) schemes. The results are shown for different length simulations; 1 time step (top left), 25 time steps (top right), 50 time steps (bottom left), and 100 time steps (bottom right).

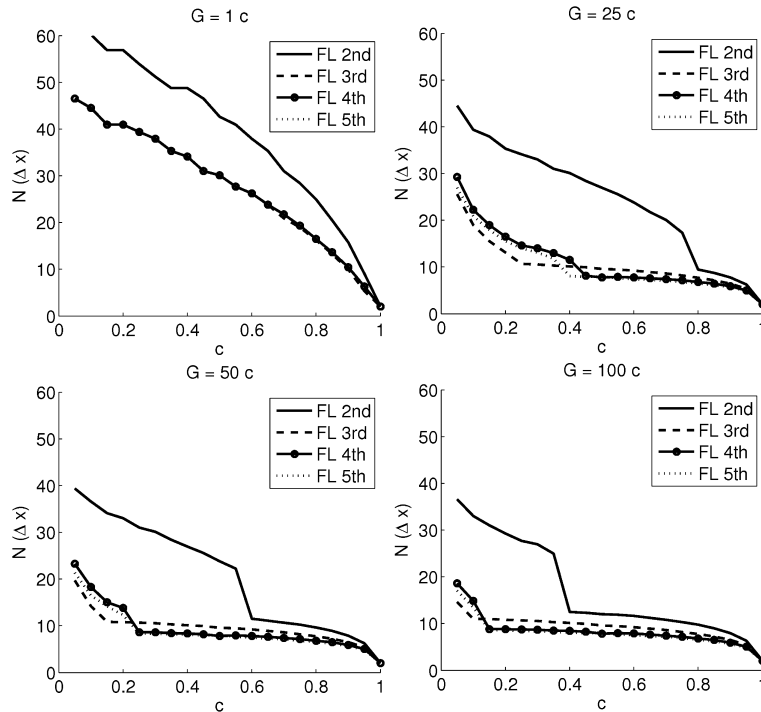


Fig. 3. Numerically calculated effective resolution, in terms of $N\Delta x$, against Courant number c , for the universal limiter used with the second (FL 2nd), third (FL 3rd), fourth (FL 4th) and fifth-order (FL 5th) forward-in-time schemes. The results are shown for different length simulations; 1 time step (top left), 25 time steps (top right), 50 time steps (bottom left), and 100 time steps (bottom right). For 1 time step (top left) the third-, fourth- and fifth-order schemes produce an almost identical effective resolution, hence the plot lines lie on top of each other.

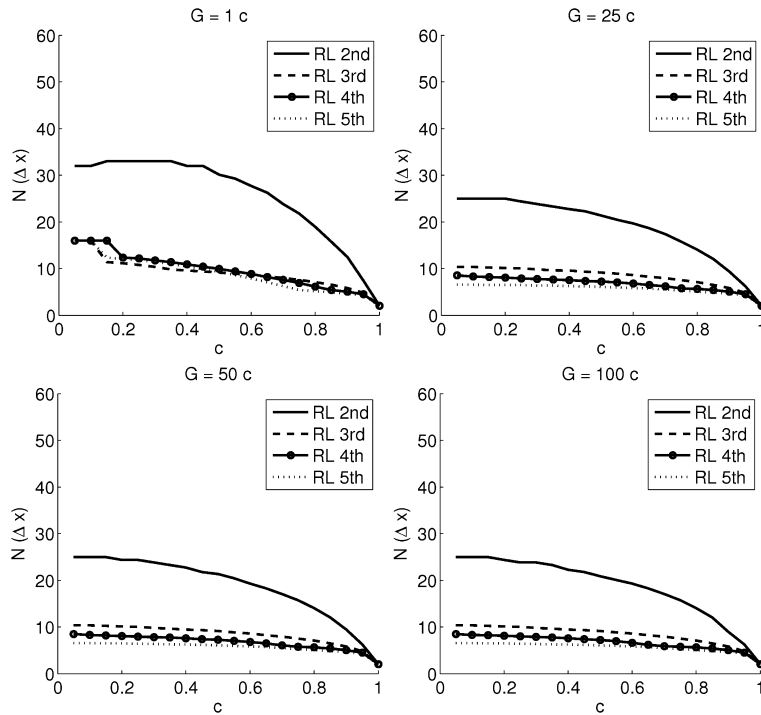


Fig. 4. Numerically calculated effective resolution, in terms of $N\Delta x$, against Courant number c , for the relaxed-limiter used with the second (RL 2nd), third (RL 3rd), fourth (RL 4th) and fifth-order (RL 5th) forward-in-time schemes. The results are shown for different length simulations; 1 time step (top left), 25 time steps (top right), 50 time steps (bottom left), and 100 time steps (bottom right).

to achieve better than third-order accuracy (regardless of the order of the unlimited scheme). Note that using the FCT algorithm with the second-, third-, fourth- and fifth-order forward-in-time schemes produces very similar results to those shown for the universal limiter in Fig. 3 (not shown).

Fig. 4 shows the effective resolution of the relaxed quasi-monotonic limiter applied to the second-, third-, fourth- and fifth-order forward-in-time schemes. As with the universal limiter, there is an initial error that affects the effective resolution at the first time step, but this is significantly smaller for the relaxed limiter than for the universal limiter. In subsequent time steps the relaxed limiter allows the scheme to behave similarly to the underlying unlimited scheme, and for 25, 50 and 100 time steps the relaxed limiter produces an almost identical effective resolution to the corresponding order unlimited forward-in-time scheme.

The final schemes we consider in this section are the PPM and WENO schemes, and their effective resolutions are shown in Fig. 5. The unlimited versions of PPM, shown in Fig. 1, are not affected by the number of time steps, and the sixth-order edge reconstruction outperforms the fourth-order edge reconstruction. Applying the limiter produces similar results to using the universal limiter (shown in Fig. 3); initially there are large errors, but the effective resolution improves as the number of time steps increases. Note that using the limiter produces very similar results for both the fourth-order and sixth-order edge reconstructions. The effective resolution for the limiter applied to PPM is worse than using the universal limiter for a similarly ordered scheme, especially for low Courant numbers. These results show the large impact that the limiter has on PPM. The WENO schemes behave similarly to the forward-in-time schemes with the relaxed quasi-monotonic limiter. Initially there is an error that produces a large effective resolution over one time step, but over many time steps the error decreases and the effective resolution becomes that of the underlying scheme. Note that the underlying scheme for the WENO schemes are not equivalent to the fourth- and fifth-order forward-in-time schemes, hence the effective resolution does not approach $2\Delta x$ as the Courant number approaches unity.

5. Conclusions

This paper is the second part in a series investigating the effective resolution of advection schemes. The effective resolution describes the smallest scale (i.e. largest wave number) that can be fully resolved by a numerical scheme. This can be calculated using dispersion analysis [8]. As this dispersion analysis can only be applied to linear schemes, we have created a numerical test strategy that calculates the effective resolution of any advection scheme, linear or non-linear. The numerical test involves advecting a tracer of wavelength k ; if the diffusive and dispersive errors fall below a given threshold then wave number k is classed as fully resolved. Comparing the numerical methodology with the analytical results from [8] shows that the numerical test can accurately determine the effective resolution. This method to numerically calculate the ef-

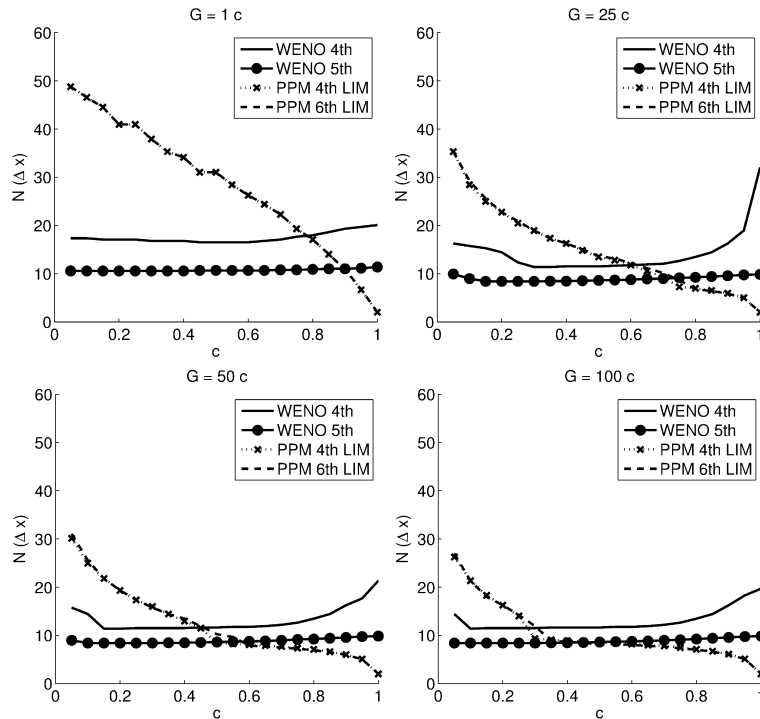


Fig. 5. Numerically calculated effective resolution, in terms of $N\Delta x$, against Courant number c , for PPM with fourth-order edge reconstruction and limiter (PPM 4th LIM), PPM with sixth-order edge reconstruction and limiter (PPM 6th LIM), fourth-order WENO (WENO 4th) and fifth-order WENO (WENO 5th). The results are shown for different length simulations; 1 time step (top left), 25 time steps (top right), 50 time steps (bottom left), and 100 time steps (bottom right). Note that the limited PPM with fourth- and sixth-order edge reconstructions produce almost identical plots.

ffective resolution is applied to one-dimensional schemes, although it is easily extendable to test two and three-dimensional schemes.

We use the numerical test to calculate the effective resolution of numerical schemes that are often used for tracer transport in dynamical cores of GCMs. Although the focus is on methods used in weather and climate models, the method and results apply to advection schemes in any area of computational fluid dynamics. We apply the test to non-linear schemes for the advection equation, and focus our attention on schemes with limiters. The results show that these schemes with non-linear limiters resolve different waves depending on how long the simulation is run. Initially, the limiters introduce large diffusion and dispersion errors, and after the first time step these schemes resolve significantly less than the corresponding unlimited scheme. As the simulation progresses the diffusion and dispersion errors grow at a slower rate for the limited schemes than the corresponding unlimited scheme.

For the second-order schemes the addition of the limiter initially reduces the effective resolution significantly, but over more time steps the effective resolution of the limited schemes improves until, for some Courant numbers, the limited schemes outperform the unlimited second-order scheme. For traditional flux limiters used with third-, fourth- and fifth-order schemes the effective resolution of the limited schemes is worse than that of the corresponding order unlimited schemes for short simulations. The effective resolution of the limited fourth- and fifth-order schemes is not a significant improvement on the limited third-order scheme, and for some simulations the third-order scheme actually has the best effective resolution of the three. This indicates that using a third-order scheme might be optimal (in terms of accuracy against cost) when using these monotonic limiters. As the length of the simulation increases the effective resolution of the limited schemes tends towards that of the corresponding order unlimited schemes. Replacing the monotonic limiter with a relaxed quasi-monotonic limiter leads to a marked improvement on the effective resolution. The errors at the initial time step are much smaller than with the monotonic limiter, and after a short time the effective resolution of the relaxed limiter reverts to that of the underlying basic unlimited scheme. The results show that using a relaxed limiter produces a better effective resolution than using a monotonic limiter for higher than third-order schemes. The tests are also performed on other types of non-linear limiter, such as the Piecewise Parabolic Method (PPM) and Weighted Essentially Non-Oscillatory (WENO) schemes. The results for the traditional flux-limiters generalize to these other limiters; the initially large error from the limiter decreases as the simulation length increases, and the use of non-monotonic limiters can produce the effective resolution of a high-order unlimited scheme.

It is worth noting that the analysis in this paper only concerns the effective resolution of a numerical advection scheme, and that although the flux limiters may reduce the effective resolution of a scheme for a short simulation, they do have other benefits. Flux limiters are used to ensure monotonicity and positivity (which is essential for tracer transport in atmo-

spheric models), and they improve the accuracy when modeling discontinuous or rough data. Also, for advection in sheared flow or for equations where there are downscale transfers of quantities from the grid scale to subgrid scales, the implicit diffusion from the flux limiters may be used as an implicit subgrid model [5,9,10,29].

Our results identify the smallest scales that can be resolved by certain advection schemes, and the impact of limiters on effective resolution for finite-difference and finite-volume schemes. These types of numerical schemes are used in all branches of computational fluid dynamics, and our focus is those that are often used in transport schemes in atmospheric models. The results show that to accurately model the transport of a trace gas, the tracer must be at a much larger scale than the grid spacing. Although this paper is only concerned with advection schemes, the results are a first step towards understanding the effective resolution of dynamical cores of atmospheric models. Many dynamical cores use methods described here, for example non-linear limiters, to solve the momentum and thermodynamic equations (for example, [18] uses a modified version of PPM), and for small Courant numbers they may be unable to fully resolve features smaller than $\approx 20\Delta x$. This means that there is a large gap between the scales resolved by the numerics that solve the dynamic equations and the grid-scale physics (and other grid-scale features such as topography).

Acknowledgements

We thank two anonymous reviewers for their constructive comments. The work was supported by the Office of Science of the U.S. Department of Energy, Award No. DE-SC0006684.

Appendix A. Relaxed quasi-monotonic limiter

This appendix briefly describes how the monotonic universal limiter [16,17] can be relaxed to create a quasi-monotonic limiter. The quasi-monotonic limiter allows higher-order accuracy for smooth data, although it does permit small over- and undershoots.

As described by [28], the universal limiter starts with a flux, q_L , at the left edge of a grid cell (in our case this is calculated by the forward-in-time schemes). The flux is limited to ensure that the updated q in the grid cell does not exceed given bounds, q_{min}^{n+1} and q_{max}^{n+1} . The relaxed limiter replaces the lower and upper cell value bounds with $q_{min}^{n+1} - \delta$ and $q_{max}^{n+1} + \delta$, where δ is small. This method does not damp the peak of smooth waves, and therefore achieves high-order accuracy when used with a high-order scheme.

To determine the value of δ we use the grid-scale violation detection method described by [37]. The flux is deemed spurious if

$$(q_L - q_{j-1})(q_j - q_L) < 0, \quad (\text{A.1})$$

and any of the following

$$(q_{j-1} - q_{j-2})(q_{j+1} - q_j) \geq 0, \quad (q_{j-1} - q_{j-2})(q_{j-2} - q_{j-3}) \leq 0,$$

$$(q_{j+1} - q_j)(q_{j+2} - q_{j+1}) \leq 0, \quad (q_L - q_{j-1})(q_{j-1} - q_{j-2}) \leq 0,$$

for grid index j . If the flux is spurious then it is limited using $\delta = 0$. If the flux is not spurious, then δ is chosen as the difference between the maximum and minimum values of (q_{j+1}, q_j, q_{j-1}) . Note that the limiter can be made positive definite by using the lower bound, $\max(q_{min}^{n+1} - \delta, 0)$.

References

- [1] J.P. Boris, D.L. Book, Flux-corrected transport I. SHASTA, a fluid algorithm that works, *J. Comput. Phys.* 11 (1973) 38–69.
- [2] P. Colella, P.R. Woodward, The Piecewise Parabolic Method (PPM) for gas-dynamical simulations, *J. Comput. Phys.* 54 (1984) 174–201.
- [3] P. Colella, M.D. Sekora, A limiter for PPM that preserves accuracy at smooth extrema, *J. Comput. Phys.* 227 (2008) 7069–7076.
- [4] S. Gottlieb, D.I. Ketcheson, C.-W. Shu, *Strong Stability Preserving Runge–Kutta and Multistep Time Discretizations*, World Scientific Publishing, New Jersey, USA, 2011.
- [5] F.F. Grinstein, L.G. Margolin, W. Rider, *Implicit Large Eddy Simulation*, Cambridge, 2007.
- [6] A. Harten, S. Osher, Uniformly high-order accurate nonoscillatory schemes. I, *SIAM J. Numer. Anal.* 24 (2) (1987) 279–309.
- [7] G.-S. Jiang, C.-W. Shu, Efficient implementation of weighted ENO schemes, *J. Comput. Phys.* 126 (1996) 202–228.
- [8] J. Kent, J.P. Whitehead, C. Jablonowski, R.B. Rood, Determining the effective resolution of advection schemes. Part I: dispersion analysis, *J. Comput. Phys.* 278 (2014) 485–496, <http://dx.doi.org/10.1016/j.jcp.2014.01.043>.
- [9] J. Kent, J. Thuburn, N. Wood, Assessing implicit large Eddy simulation for two-dimensional flow, *Q. J. R. Meteorol. Soc.* 138 (2012) 365–375.
- [10] J. Kent, C. Jablonowski, J.P. Whitehead, R.B. Rood, Downscale cascades in tracer transport test cases: an intercomparison of the dynamical cores in the Community Atmosphere Model CAM5, *Geosci. Model Dev.* 5 (2012) 1517–1530.
- [11] J.-F. Lamarque, D.E. Kinnison, P.G. Hess, F.M. Vitt, Simulated lower stratospheric trends between 1970 and 2005: identifying the role of climate and composition changes, *J. Geophys. Res.* 113 (2008) D12301, <http://dx.doi.org/10.1029/2007JD009277>.
- [12] J. Lander, B.J. Hoskins, Believable scales and parameterizations in a spectral transform model, *Mon. Weather Rev.* 125 (1997) 292–303.
- [13] P.H. Lauritzen, P.A. Ullrich, R.D. Nair, Atmospheric Transport Schemes: desirable properties and a semi-Lagrangian view on finite-volume discretizations, in: P.H. Lauritzen, C. Jablonowski, M.A. Taylor, R.D. Nair (Eds.), *Numerical Techniques for Global Atmospheric Models*, Springer, 2011, pp. 187–254.
- [14] P.H. Lauritzen, A stability analysis of finite-volume advection schemes permitting long time steps, *Mon. Weather Rev.* 135 (2007) 2658–2673.
- [15] P.D. Lax, B. Wendroff, Systems of conservation laws, *Commun. Pure Appl. Math.* 13 (1960) 217–237.

- [16] B.P. Leonard, The ULTIMATE conservative difference scheme applied to unsteady one-dimensional advection, *Comput. Methods Appl. Mech. Eng.* 88 (1991) 17–74.
- [17] B.P. Leonard, Universal limiter for transient interpolation modeling of the advective transport equations: the ULTIMATE conservative difference scheme, NASA Technical Memorandum 100916, 1988, p. 115.
- [18] S.J. Lin, A “vertically Lagrangian” finite-volume dynamical core for global models, *Mon. Weather Rev.* 132 (2004) 2293–2307.
- [19] X.-D. Liu, S. Osher, T. Chan, Weighted essentially non-oscillatory schemes, *J. Comput. Phys.* 115 (1994) 200–212.
- [20] D. Long, J. Thuburn, Numerical wave propagation on non-uniform one-dimensional staggered grids, *J. Comput. Phys.* 230 (2011) 2643–2659.
- [21] T. Melvin, A. Staniforth, J. Thuburn, Dispersion analysis of the spectral element method, *Q. J. R. Meteorol. Soc.* 138 (2012) 1934–1947, <http://dx.doi.org/10.1002/qj.1906>.
- [22] M. Ovtchinnikov, R.C. Easter, Nonlinear advection algorithms applied to interrelated tracers: errors and implications for modeling aerosol–cloud interactions, *Mon. Weather Rev.* 137 (2009) 632–644.
- [23] R.B. Rood, Numerical advection algorithms and their role in atmospheric transport and chemistry models, *Rev. Geophys.* 25 (1987) 71–100.
- [24] W.C. Skamarock, A linear analysis of the NCAR CCSM finite-volume dynamical core, *Mon. Weather Rev.* 136 (2008) 2112–2119.
- [25] A. Staniforth, J. Cote, Semi-Lagrangian integration schemes for atmospheric models – a review, *Mon. Weather Rev.* 119 (1991) 2206–2223.
- [26] P.K. Sweby, High resolution schemes using flux limiters for hyperbolic conservation laws, *SIAM J. Numer. Anal.* 21 (5) (1984) 995–1011.
- [27] L. Takacs, A two-step scheme for the advection equation with minimized dissipation and dispersion error, *Mon. Weather Rev.* 113 (1985) 1050–1065.
- [28] J. Thuburn, Multidimensional flux-limited advection schemes, *J. Comput. Phys.* 23 (1996) 74–83.
- [29] J. Thuburn, Dissipation and cascades to small scales in numerical models using a shape-preserving advection scheme, *Mon. Weather Rev.* 123 (1994) 1888–1903.
- [30] E.F. Toro, R.C. Millington, L.A.M. Nejad, Towards very high order Godunov schemes, in: E.F. Toro (Ed.), *Godunov Methods: Theory and Applications*, Kluwer Academic/Plenum Publishers, New York, 2001, pp. 907–940.
- [31] C.J. Tremback, J. Powell, W.R. Cotton, R.A. Pielke, The forward-in-time upstream advection scheme: extension to higher orders, *Mon. Weather Rev.* 115 (1987) 540–555.
- [32] P.A. Ullrich, Understanding the treatment of waves in atmospheric models. Part 1: the shortest resolved waves of the 1D linearized shallow-water equations, *Q. J. R. Meteorol. Soc.* 140 (2014) 1426–1440, <http://dx.doi.org/10.1002/qj.2226>.
- [33] B. Van Leer, Towards the ultimate conservative difference scheme, II. Monotonicity and conservation combined in a second order scheme, *J. Comput. Phys.* 14 (1974) 361–370.
- [34] M.K. Walters, Comments on “The differentiation between grid spacing and resolution and their application to numerical modeling”, *Bull. Am. Meteorol. Soc.* 81 (2000) 2475–2477.
- [35] J.P. Whitehead, C. Jablonowski, R.B. Rood, P.H. Lauritzen, A stability analysis of divergence damping on a latitude–longitude grid, *Mon. Weather Rev.* 139 (2011) 2976–2993.
- [36] D.L. Williamson, Equivalent finite volume and Eulerian spectral transform horizontal resolutions established from aqua-planet simulations, *Tellus* 60A (2008) 839–847.
- [37] M. Zerroukat, N. Wood, A. Staniforth, A monotonic and positive-definite filter for a Semi-Lagrangian Inherently Conserving and Efficient (SLICE) scheme, *Q. J. R. Meteorol. Soc.* 131 (2005) 2933–2936.